Diabetologia (2012) 55:3369–3381
DOI 10.1007/s00125-012-2720-0

ARTICLE

Enhanced phosphoinositide 3-kinase(p110α) activity prevents diabetes-induced cardiomyopathy and superoxide generation in a mouse model of diabetes

R. H. Ritchie · J. E. Love · K. Huynh · B. C. Bernardo · D. C. Henstridge · H. Kiriazis · Y. K. Tham · G. Sapra · C. Qin · N. Cemerlang · E. J. H. Boey · K. Jandeleit-Dahm · X.-J. Du · J. R. McMullen

Received: 27 May 2012 / Accepted: 10 August 2012 / Published online: 22 September 2012

Abstract
Aims/hypothesis Diabetic cardiomyopathy is characterised by diastolic dysfunction, oxidative stress, fibrosis, apoptosis and pathological cardiomyocyte hypertrophy. Phosphoinositide 3-kinase (PI3K)(p110α) is a cardioprotective kinase, but its role in the diabetic heart is unknown. The aim of this study was to assess whether PI3K(p110α) plays a critical role in the induction of diabetic cardiomyopathy, and whether increasing PI3K(p110α) activity in the heart can prevent the development of cardiac dysfunction in a setting of diabetes.

Methods Type 1 diabetes was induced with streptozotocin in adult male cardiac-specific transgenic mice with increased PI3K(p110α) activity (constitutively active PI3K [p110α], caPI3K] or decreased PI3K(p110α) activity (dominant-negative PI3K [p110α], dnPI3K) and non-transgenic (Ntg) mice for 12 weeks. Cardiac function, histological and molecular analyses were performed.

Results Diabetic Ntg mice displayed diastolic dysfunction and increased cardiomyocyte size, expression of atrial and B-type natriuretic peptides (*Anp*, *Bnp*), fibrosis and apoptosis, as well as increased superoxide generation and increased protein kinase C β2 (PKCβ2), $p22^{phox}$ and apoptosis signal-regulating kinase 1 (*Ask1*) expression. Diabetic dnPI3K mice displayed an exaggerated cardiomyopathy phenotype compared with diabetic Ntg mice. In contrast, diabetic caPI3K mice were protected against diastolic dysfunction, pathological cardiomyocyte hypertrophy, fibrosis and apoptosis. Protection in diabetic caPI3K mice was associated with attenuation of left ventricular superoxide generation, attenuated *Anp*, *Bnp*, PKCβ2, *Ask1* and $p22^{phox}$ expression, and elevated AKT. Further, in cardiomyocyte-like cells, increased PI3K(p110α) activity suppressed high glucose-induced superoxide generation and enhanced mitochondrial function.

Conclusions/interpretation These results demonstrate that reduced PI3K activity accelerates the development of diabetic cardiomyopathy, and that enhanced PI3K(p110α) activity can prevent adverse cardiac remodelling and dysfunction in a setting of diabetes.

Keywords Diabetes · Fibrosis · Hypertrophy · Left ventricular function · Myocardium · NADPH oxidase · PI3K · PKCβ2 · Reactive oxygen species

Electronic supplementary material The online version of this article (doi:10.1007/s00125-012-2720-0) contains peer-reviewed but unedited supplementary material, which is available to authorised users.

J. E. Love and K. Huynh contributed equally to this study.

R. H. Ritchie (✉) · J. E. Love · K. Huynh · B. C. Bernardo · D. C. Henstridge · H. Kiriazis · Y. K. Tham · G. Sapra · C. Qin · N. Cemerlang · E. J. H. Boey · K. Jandeleit-Dahm · X.-J. Du · J. R. McMullen (✉)
Baker IDI Heart and Diabetes Institute,
PO Box 6492, St Kilda Rd Central,
Melbourne, VIC 8008, Australia
e-mail: rebecca.ritchie@bakeridi.edu.au
e-mail: Julie.mcmullen@bakeridi.edu.au

R. H. Ritchie · K. Huynh · X.-J. Du · J. R. McMullen
Department of Medicine, Monash University,
Clayton, VIC, Australia

J. R. McMullen
Department of Physiology, Monash University,
Clayton, VIC, Australia

Abbreviations

ASK1	Apoptosis signal-regulating kinase 1
BAX	Bcl-2-associated X protein
BCL2	B cell lymphoma 2
caPI3K	Constitutively active phosphoinositide 3-kinase, p110α isoform
dnPI3K	Dominant-negative phosphoinositide 3-kinase, p110α isoform
dP/dt_{min}	Minimum rate of left ventricular pressure change
E/A ratio	Ratio of initial and second blood flow velocities
HG	High glucose
HW	Heart weight
IVRT	Isovolumic relaxation time
LG	Low glucose
LV	Left ventricular
LVEDP	Left ventricular end-diastolic pressure
NRVM	Neonatal rat ventricular myocytes
Ntg	Non-transgenic
PI3K	Phosphoinositide 3-kinase
PI3K(p110α)	Phosphoinositide 3-kinase, p110α isoform
PKCβ2	Protein kinase C, β2 isoform
rAAV	Recombinant adeno-associated viral (vector)
ROS	Reactive oxygen species
STZ	Streptozotocin
Tg	Transgenic
TL	Tibial length
UCP3	Uncoupling protein 3

Introduction

The incidence of diabetes is rising globally and diabetes is predicted to affect 439–472 million adults by 2030 [1, 2]. Diabetes is associated with increased mortality and morbidity, attributed largely to cardiovascular and kidney disease [3, 4]. Diabetic cardiomyopathy, both independent of and exacerbated by coexistent atherosclerosis, coronary disease and renal dysfunction, is characterised by structural and functional remodelling, including diastolic dysfunction, fibrosis, apoptosis and pathological cardiomyocyte hypertrophy [3, 4]. Oxidative stress, an imbalance between reactive oxygen species (ROS) generation and endogenous antioxidant capacity, is triggered in cardiomyocytes by hyperglycaemia. This contributes to the development and progression of diabetic cardiomyopathy [5–8]. The superoxide-generating enzyme NADPH oxidase is considered a major source of ROS in the heart [9].

Current glucose-lowering agents do not consistently reduce cardiovascular risk, and some may even increase it [10, 11]. Thus, new therapeutic strategies to protect the heart in the setting of diabetes are greatly needed. We have previously demonstrated that increased activation of phosphoinositide 3-kinase (PI3K)(p110α) in the heart is protective in pathological settings in which the heart is subjected to a localised cardiac insult such as aortic constriction (pressure overload) or coronary artery ligation (myocardial infarction) [12–14]. However, whether PI3K (p110α) can protect the heart against diabetic cardiomyopathy caused by global hyperglycaemia is unknown. Furthermore, PI3K has previously been linked to ROS inhibition in the kidney [15], but whether PI3K can regulate cardiac ROS has not been elucidated.

Multiple signalling proteins/cascades are dysregulated in the diabetic heart, including extracellular signal-regulated kinase 1 (ERK1), signal transducer and activator of transcription 3 (STAT3) and AKT (a key downstream target of PI3K) [4, 16–19]. A critical step in developing better therapeutics is to understand which signalling events represent key mechanisms in the development of cardiomyopathy in a setting of hyperglycaemia. The goal of the current study was to assess whether PI3K(p110α) plays a critical role in the induction of diabetic cardiomyopathy, and whether increasing PI3K(p110α) activity in the mouse heart prevents the development of diabetes-induced left ventricular (LV) remodelling and dysfunction.

Methods

Mouse models The Alfred Medical Research and Education Precinct Animal Ethics Committee approved animal care and experimentation. Cardiomyocyte-specific transgenic (Tg) mice (FVB/N background) with increased PI3K (p110α) activity (constitutively active PI3K [p110α], caPI3K) or decreased PI3K(p110α) activity (dominant-negative PI3K [p110α], dnPI3K) were originally generated and provided by S. Izumo (Beth Israel Deaconess Medical Center, Boston, MA, USA) [20]. Compared with non-transgenic (Ntg) mice, caPI3K-Tg mice have elevated cardiac PI3K(p110α) activity, normal cardiac function and hearts that are 20% larger (physiological hypertrophy) [20], while dnPI3K-Tg mice have reduced cardiac PI3K(p110α) activity, normal cardiac function and hearts that are 20% smaller.

Male caPI3K-Tg, dnPI3K-Tg and Ntg mice were randomly allocated into diabetic and non-diabetic groups. At 6–7 weeks of age, mice received five consecutive daily i.p. injections of streptozotocin (STZ, 55 mg/kg body weight, in 0.1 mol/l citrate buffer, pH4.5; Sigma-Aldrich, St Louis, MO, USA) to induce diabetes or five consecutive daily i.p. injections of citrate buffer vehicle of equivalent volume (non-diabetic group) [21]. Diabetes was confirmed by measuring blood glucose every 2 weeks from saphenous vein whole blood using a glucometer (ACCU-CHEK Advantage; Roche, Basel, Switzerland). The upper limit of detection for

blood glucose readings was 33.3 mmol/l; readings at this level were entered as 33.3 mmol/l and confirmed by subsequent submandibular bleed from conscious mice for assessment of the final plasma glucose level (Austin Pathology Service, Heidelberg, VIC, Australia). Mice with blood glucose levels exceeding 28 mmol/l were considered diabetic. Diabetes progressed untreated for 12 weeks. At the endpoint of the study (≈18–19 weeks of age), whole blood was collected by cardiac puncture after cardiac catheterisation for analysis of HbA_{1c} (Austin Pathology Service).

LV function Echocardiography (two-dimensional M-mode and Doppler flow) was performed in anaesthetised mice (ketamine/xylazine/atropine: 100/10/1.2 mg/kg i.p.) prior to catheterisation and mouse dissection (≈18–19 weeks of age) utilising a Philips iE33 ultrasound machine (North Ryde, NSW, Australia) with a 15 MHz linear array transducer, as previously described [21]. LV posterior wall thickness, LV chamber dimensions and fractional shortening were assessed. LV filling was assessed on transmitral Doppler echocardiography, the ratio of initial (E) and second (A) blood flow velocities (E/A ratio), E velocity deceleration time and isovolumic relaxation time (IVRT).

Haemodynamic variables were examined after 12 weeks of diabetes by catheterisation. Arterial pressures, LV systolic pressure, LV end-diastolic pressure (LVEDP), maximum and minimum (dP/dt_{min}) rates LV pressure change and heart rate were measured in anaesthetised mice (ketamine/xylazine/atropine: 100/10/1.2 mg/kg i.p.) using a 1.4 Fr Millar MIKRO-TIP catheter and a PowerLab System (AD Instruments, Bella Vista, NSW, Australia) [21].

Tissue collection and histological and immunohistochemical analyses Following cardiac catheterisation, heart, lung and tibia were collected [21]. Ventricular sections (4 μm) were stained with haematoxylin and eosin for assessment of cardiomyocyte width or with 0.1% Picrosirius Red for assessment of collagen deposition, as previously described [21]. Apoptosis was detected in paraffin-embedded ventricular sections (4 μm) by TUNEL staining (CardioTACS In Situ Apoptosis Detection Kit; Trevigen, Gaithersburg, MD, USA). Apoptotic nuclei were stained blue and quantified as a percentage of non-apoptotic nuclei (counterstained red with Nuclear Fast Red) and expressed as a fold-change of non-diabetic Ntg mice.

For immunohistochemical examination of $p22^{phox}$, paraffin-embedded ventricular sections (4 μm) were deparaffinised and rehydrated, and antigen retrieval was induced by heat (100°C) in a citrate buffer (10 mmol/l citric acid, 0.05% Tween-20, pH6.0). Endogenous peroxidase activity was quenched (3% H_2O_2 [vol./vol.]) and sections were blocked (15 μl/ml normal goat serum in 1% BSA) and stained with $p22^{phox}$ (sc-20781, 1:100; Santa Cruz Biotechnology, Santa Cruz, CA, USA) overnight, followed by biotinylated secondary goat α-rabbit IgG (1:200; Vector Laboratories, Burlingame, CA, USA). After exposure to VECTASTAIN Elite ABC avidin-biotinylated horseradish peroxidase complex (Vector Laboratories), the chromogenic reaction was carried out with Sigma-FAST diaminobenzidine tablets (Sigma-Aldrich). Sections were counterstained with haematoxylin. Positive $p22^{phox}$ stained brown and was graded by a blinded observer as follows: score 0, negative stain; score 1, weak; score 2, moderate; score 3, strong/intense.

Superoxide generation Generation of superoxide was assessed in fresh LV tissue, neonatal rat ventricular myocytes (NRVM) or H9c2 cells using lucigenin-enhanced chemiluminescence, as previously described [22]. Primary NRVM [22] or H9c2 cells (Cell Bank Australia, Westmead, NSW, Australia) were plated for 72 or 18 h, respectively, in 96 well OptiView plates (50,000 and 5,000 cells/well, respectively, 37°C/5% CO_2), serum-deprived for approximately 18 h and pretreated with or without a specific PI3K(p110α) inhibitor (A66 [23], 1 μmol/l), IGF1 (10 nmol/l) and/or tempol (100 μmol/l) for 24 h prior to 24 h treatment with or without H_2O_2 (100 μmol/l) in high glucose (HG, 25 mmol/l) or low glucose (LG, 5.56 mmol/l) media, as specified.

Mitochondrial function H9c2 cells were seeded into Seahorse plates (10,000 cells/well in HG: 25 mmol/l), serum-deprived overnight and treated with IGF1 (10 nmol/l) and/or A66 (10 μmol/l) for 24 h, followed by assessment of mitochondrial function (Seahorse Bioscience XF Analyser, North Billerica, MA, USA). Following basal respiration measurements, cells were sequentially treated with (all 1 μmol/l) oligomycin (ATP synthase inhibitor), carbonyl cyanide p-trifluoromethoxyphenylhydrazone (FCCP, proton ionophore) and antimycin A/rotenone combination injection (inhibitors of complex I and III), and changes in respiration were recorded. Treatments were analysed as ten replicates over two independent experiments (plates) and data were pooled to give average values for each treatment. Basal respiration, proton leak, ATP turnover, spare respiratory capacity and maximal respiratory capacity were calculated from these analyses.

RNA and protein extraction RNA and protein were extracted from frozen ventricle samples as previously described [21].

Northern blot analysis Northern blot analysis was performed as previously reported [20]. Total RNA (10 μg) was electrophoresed in 1.3% denaturing formaldehyde-agarose gels and blotted onto Hybond–N membranes (GE Healthcare, Rydalmere. NSW, Australia). Membranes were probed with *Anp* (also known as *Nppa*), *Bnp* (also known as *Nppb*), *$p22^{phox}$* (also known as *Cyba*), *Ask1* (also known as

Map3k5), *Ucp3*, *Pim1*, *Tfam*, and *Gapdh* radiolabelled probes. Details of northern probes are presented in the electronic supplementary material (ESM).

Western blotting For pAKT, blots were probed with anti-phospho (p)AKT antibody (Ser473, Cell Signaling Technologies, Danvers, MA, USA: 9271, 1:500) followed by anti-AKT antibody (Cell Signaling: 9272, 1:1,000). For BAX (Bcl-2-associated X protein) and BCL2 (B cell lymphoma 2), blots were probed with anti-BAX antibody (Cell Signaling: 2772, 1:1,000) followed by anti-BCL2 antibody (Cell Signaling: 2876, 1:1,000). For protein kinase C β2 (PKCβ2) and uncoupling protein 3 (UCP3), blots were probed with anti-PKCβ2 (sc-210,1:200; Santa Cruz Biotechnology) and anti-UCP3 antibody (PA1-065, 1:1,000; ABR Affinity BioReagents, Golden, CO, USA), both followed by anti-GAPDH antibody (sc-32233, 1:5,000; Santa Cruz Biotechnology).

Statistical analysis Results are presented as mean ± standard error. Differences between groups were compared using one-way ANOVA followed by the Fisher's protected least significant difference, unless otherwise specified. $p<0.05$ was considered significant.

Results

Induction of diabetes in Ntg and PI3K Tg mice STZ induced a comparable degree of diabetes in Ntg, dnPI3K and caPI3K mice. Blood glucose, plasma glucose and HbA_{1c} levels increased to a similar extent in STZ-treated mice from each genotype compared with citrate-treated non-diabetic controls (Table 1). No genotype-dependent differences in glycaemia, body weight or tibial length (TL) were observed (Table 1).

Increased PI3K(p110α) activity prevents diabetes-induced increases in cardiomyocyte size, fibrosis and apoptosis Cardiomyocyte hypertrophy, fibrosis and apoptosis all contribute to the pathogenesis and progression of diabetic cardiomyopathy [24, 25]. Induction of diabetes in Ntg mice for 12 weeks had no impact on heart weight (HW; see HW/TL, Table 1) but was associated with increased cardiomyocyte width (≈13%; Fig. 1a–c), increased *Anp* and *Bnp* cardiac gene expression (markers of pathological hypertrophy and/or cardiac stress; Fig. 1d), cardiac fibrosis (Fig. 2a) and increased apoptosis (Fig. 2b). A diabetes-induced increase in cardiomyocyte size in the absence of a parallel increase in heart size is consistent with previous findings [21] and can be attributed to increased cell death in the diabetic heart (Fig. 2b) [26].

Under basal/non-diabetic conditions, caPI3K-Tg mice displayed physiological cardiac hypertrophy associated with larger cardiomyocytes compared with Ntg, but no increase in *Anp* or *Bnp* expression, as previously reported (Table 1, see HW, HW/TL; Fig. 1a, b, d) [20]. In contrast, non-diabetic dnPI3K-Tg mice had smaller hearts, smaller cardiomyocytes and elevated *Anp* and *Bnp* expression (Table 1, Fig. 1a, b, d) [20]. Neither caPI3K-Tg nor dnPI3K-Tg mice showed evidence of fibrosis or apoptosis under basal/non-diabetic conditions (Fig. 2a, b). Diabetes had no effect on HW/TL in caPI3K-Tg or dnPI3K-Tg mice (Table 1). However, PI3K activity had a significant impact on cardiomyocyte size, fibrosis and apoptosis in a setting of diabetes that differed from diabetic Ntg mice. Expression of the dn*PI3K* transgene was associated with an exaggerated diabetes-induced increase in cardiomyocyte size compared

Table 1 Systemic and morphological characteristics of Ntg and PI3K non-diabetic and diabetic mouse models

Variable	Ntg		dnPI3K		caPI3K	
	Non-diabetic	Diabetic	Non-diabetic	Diabetic	Non-diabetic	Diabetic
n	11	12	7	7	6	8
Blood glucose (mmol/l)	11.3±0.3	33.2±0.1*	11.3±0.5	33.3±0.0*	11.0±0.7	32.8±0.6*
Plasma glucose (mmol/l)	8.6±0.4 (*n*=6)	33.3±1.7* (*n*=10)	7.9±0.9 (*n*=5)	34.1±1.7* (*n*=6)	8.4±0.3	31.2±2.1*
HbA_{1c} (%)	3.8±0.5 (*n*=6)	9.3±0.3* (*n*=10)	3.9±0.7 (*n*=5)	8.9±0.3* (*n*=5)	3.2±0.3	9.9±0.4*
HbA_{1c} (mmol/mol)	17.7±5.3 (*n*=6)	78.0±3.7* (*n*=10)	18.7±7.3 (*n*=5)	74.2±3.6* (*n*=5)	11.8±3.7	84.2±3.9*
Body weight (g)	32.9±1.3	29.8±0.8	31.2±1.6	29.3±0.8	30.2±1.3	28.7±1.0
TL (mm)	16.7±0.1	16.5±0.1	16.6±0.2	16.2±0.2	16.3±0.3	16.2±0.2
HW (mg)	133.1±3.4	122.3±4.2	105.0±7.2†	98.9±2.3†	147.2±6.0‡§	149.3±6.4†‡
Lung weight (mg)	148.0±3.8	155.3±4.6	155.6±8.8	153.0±6.9	140.7±4.5	139.5±5.9
HW/TL (mg/mm)	7.96±0.18	7.41±0.23	6.31±0.38†	6.10±0.10†	9.05±0.31†‡	9.19±0.31†‡

*$p<0.05$ vs non-diabetic mice of the same genotype; †$p<0.05$ vs Ntg non-diabetic mice; ‡$p<0.05$ vs dnPI3K non-diabetic mice; §$p=0.06$ vs Ntg non-diabetic mice

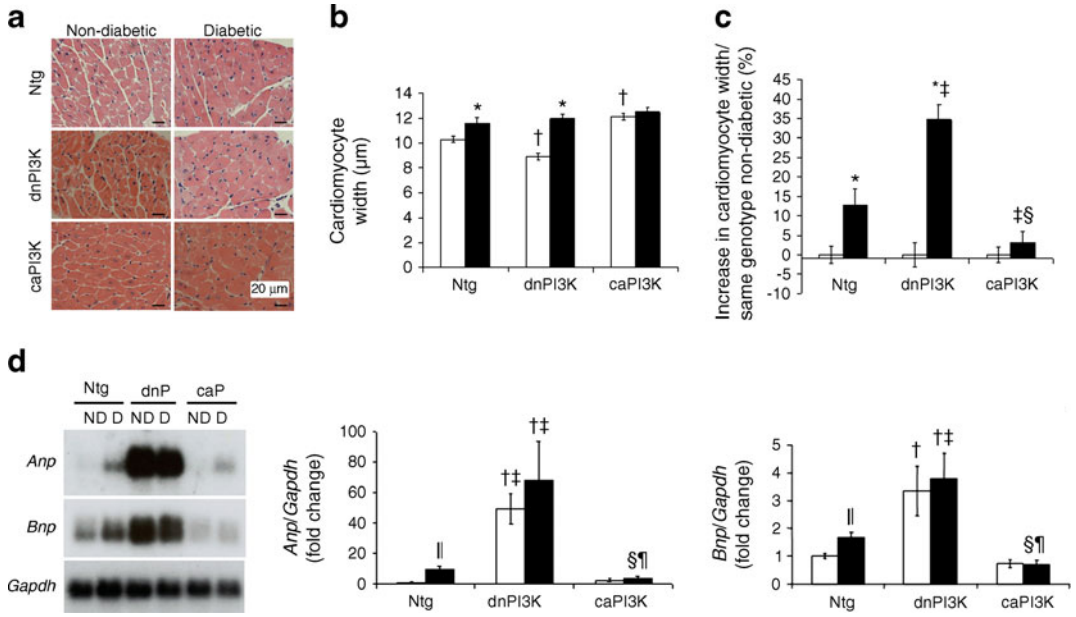

Fig. 1 The diabetes-induced increase in cardiomyocyte width is exaggerated in dnPI3K mice and attenuated in caPI3K mice. (**a**) Representative LV sections stained with haematoxylin and eosin from non-diabetic and diabetic Ntg, dnPI3K and caPI3K mice (magnification ×400); scale bars, 20 μm. (**b**) Quantitative analysis of cardiomyocyte width. (**c**) Per cent increase in cardiomyocyte width in comparison with non-diabetic mice of the same genotype. (**b**, **c**) n=5–11 per group. (**d**) Representative northern blot showing gene expression of *Anp* and *Bnp* in hearts from Ntg, dnPI3K (dnP) and caPI3K (caP) mice. *Gapdh* was used to normalise for RNA loading. Quantitative analyses (n=4–6 per group; D, diabetic; ND, non-diabetic). Mean values for non-diabetic Ntg mice were normalised to 1. White bars, non-diabetic; black bars, diabetic. *p<0.05 vs non-diabetic mice of the same genotype; †p<0.05 vs non-diabetic Ntg mice; ‡p<0.05 vs diabetic Ntg mice; §p<0.05 vs diabetic dnPI3K mice; ‖p≤0.05 vs non-diabetic Ntg mice (unpaired t test); ¶p=0.05 vs diabetic Ntg mice (unpaired t test)

with Ntg mice (≈35% in dnPI3K vs ≈13% in Ntg mice), whereas expression of the ca*PI3K* transgene prevented any significant increase in cardiomyocyte size in a setting of diabetes (Fig. 1a–c). There was no increase in *Anp* or *Bnp* expression in the hearts of diabetic caPI3K-Tg mice, consistent with the suggestion that increased PI3K activity prevents pathological cardiomyocyte growth (Fig. 1d). Furthermore, fibrosis, apoptosis and the BAX/BCL2 ratio (apoptotic marker) were significantly increased in the hearts of diabetic dnPI3K-Tg but not diabetic caPI3K-Tg mice (Fig. 2a–c). Increased apoptosis in diabetic dnPI3K-Tg mice is likely to account for the absence of an increase in HW/TL despite the increase in cardiomyocyte size in diabetic dnPI3K-Tg mice. Protection against fibrosis and apoptosis in caPI3K diabetic hearts was associated with enhanced AKT phosphorylation (Fig. 2d). pAKT/total AKT was not elevated in Ntg or dnPI3K hearts under non-diabetic or diabetic conditions. Gene expression of *Pim1* (a kinase that mediates protection downstream of AKT) was elevated in Ntg and caPI3K hearts in response to diabetes, but not in dnPI3K hearts (Fig. 2e).

Enhanced PI3K(p110α) activity protects the heart against diabetes-induced cardiac dysfunction Non-diabetic caPI3K-Tg mice had thicker LV walls than non-diabetic Ntg and dnPI3K-Tg mice, reflecting the development of physiological hypertrophy (Table 2, see LV posterior wall thickness), as previously shown [20]. In contrast, dnPI3K-Tg mice had thinner walls than Ntg mice (Table 2). At comparable heart rates, there were no significant differences in systolic or diastolic function in non-diabetic Ntg, caPI3K-Tg or dnPI3K-Tg mice (Table 2). The model of diabetes used in the current study has previously been shown to induce diastolic but not systolic dysfunction [21], consistent with the clinical context of the diabetic heart [3, 4]. In the current study, diabetes did not suppress fractional shortening in Ntg mice; interestingly fractional shortening was significantly higher in diabetic caPI3K-Tg than in diabetic Ntg and diabetic dnPI3K-Tg mice (Table 2). Aortic and LV systolic pressures were lower in diabetic Ntg and diabetic dnPI3K-Tg mice compared with their non-diabetic counterparts, but not in diabetic caPI3K-Tg mice (Table 2). The maximum rate of LV pressure change (a marker of LV systolic function) was not different between the six groups (Table 2).

Diabetic Ntg mice displayed diastolic dysfunction, as shown by reduced LV dP/dt_{min} (≈10%, Fig. 3a) and elevated LVEDP (≈87%, Fig. 3b). The increased LVEDP was exaggerated in diabetic dnPI3K-Tg compared with non-diabetic dnPI3K-Tg mice (≈119%), and was greater than that found in diabetic Ntg mice (Fig. 3b). There was also a fall in dP/dt_{min} in diabetic dnPI3K-Tg compared with non-diabetic

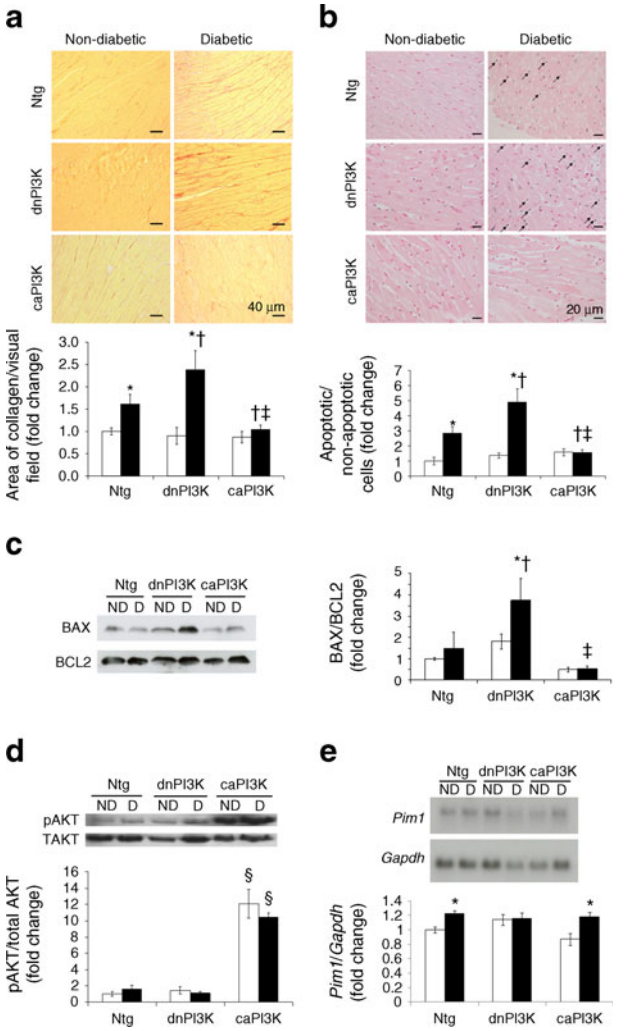

Fig. 2 PI3K(p110α) provides protection against fibrosis and apoptosis. (**a**) Representative LV sections from non-diabetic and diabetic Ntg, dnPI3K and caPI3K mice, showing collagen deposition/fibrosis in red (Sirius Red stain; magnification ×200; scale bars 40 μm), and quantitative analysis of collagen area/total ventricular area (fold change vs non-diabetic Ntg mice) (n=4–13 per group). (**b**) Representative LV sections labelled with TUNEL staining. Positively stained apoptotic cells appear dark blue (arrows). Magnification ×200; scale bars, 20 μm. Quantitation of positively stained apoptotic cells/negatively stained non-apoptotic cells, fold non-diabetic Ntg mice, n=4–7 per group. (**c**) Representative western blot showing BAX and BCL2 in hearts of non-diabetic (ND) and diabetic (D) mice and quantitative analysis of BAX/BCL2 ratio. Mean values for non-diabetic Ntg mice were normalised to 1 (n=3–4 per group). (**d**) Representative western blot showing pAKT and total AKT, and quantitative analysis of AKT phosphorylation normalised to total AKT (n=3–6 per group). (**e**) Representative northern blot showing gene expression of *Pim1* and *Gapdh*, and quantitative analyses (n=3–4 per group). White bars, non-diabetic; black bars, diabetic. *p< 0.05 vs non-diabetic mice of the same genotype; †p<0.05 vs diabetic Ntg mice; ‡p<0.05 vs diabetic dnPI3K mice; §p<0.05 vs non-diabetic and diabetic Ntg and dnPI3K mice

dnPI3K-Tg mice (Fig. 3a). By contrast, there were no significant differences in dP/dt_{min} or LVEDP between diabetic caPI3K-Tg and non-diabetic caPI3K-Tg mice (Fig. 3a, b). Diastolic function was also assessed by measuring transmitral valve flow velocities during early and late diastolic filling. This is the first study to investigate the impact of the dn*PI3K* transgene on transmitral flow, under either basal or diabetic conditions. Non-diabetic dnPI3K-Tg mice displayed abnormal patterns of mitral flow (Fig. 3c). As a result, E/A ratios in dnPI3K mice were very distinct from those observed in non-diabetic Ntg and caPI3K-Tg mice (Fig. 3d). The reason for this novel functional phenotype is currently unclear and requires further investigation. We demonstrate, however, that diabetes was associated with a fall in the E/A ratio in Ntg and dnPI3K-Tg mice, but not in caPI3K-Tg mice (Fig. 3d). Furthermore, diabetes was associated with a prolongation in deceleration time and IVRT in Ntg and dnPI3K-Tg mice, but a smaller or no rise in caPI3K-Tg mice (Fig. 3e, f). Collectively, these data suggest that the ca*PI3K* transgene can preserve diastolic function in a setting of diabetes.

Increased PI3K(p110α) activity prevents superoxide generation in a setting of diabetes and can improve mitochondrial function Hyperglycaemia promotes ROS production in many tissues, contributing to the pathogenesis of multiorgan damage in diabetes [7]. The superoxide-generating NADPH oxidase is a key source of ROS in the heart [27, 28]. Diabetes induced an increase in cardiac superoxide generation by approximately 90% in Ntg compared with non-diabetic Ntg mice (Fig. 4a). Interestingly, superoxide was increased to a similar degree in non-diabetic dnPI3K-Tg mice and there was no further increase in a setting of diabetes. By contrast, superoxide generation was similar in hearts from non-diabetic Ntg and caPI3K-Tg mice, and there was no increase in hearts of diabetic caPI3K-Tg mice (Fig. 4a). A large body of evidence has demonstrated that hyperglycaemia leads to activation of PKCβ2 in the heart and subsequent activation of NADPH oxidase [29]. PKCβ2 protein production was increased in diabetic Ntg hearts compared with non-diabetic Ntg hearts (Fig. 4b) and increased further in diabetic dnPI3K hearts, but was not significantly increased in diabetic caPI3K hearts (Fig. 4b). Gene expression of $p22^{phox}$ and *Ask1* was also elevated in hearts of diabetic Ntg vs non-diabetic Ntg mice (Fig. 4c). As observed with LV superoxide generation, $p22^{phox}$ and *Ask1* expression levels were elevated in hearts of dnPI3K-Tg mice regardless of diabetic status, but were not increased in hearts from diabetic caPI3K-Tg mice (Fig. 4c). Immunohistochemistry analysis of $p22^{phox}$ production was consistent with gene expression data (Fig. 4d).

Superoxide generation was also assessed in NRVM and the cardiomyoblast H9c2 cell line to assess whether acute activation of PI3K(p110α) with IGF1 (an upstream regulator) would inhibit HG-induced superoxide (as occurred in the caPI3K heart), and whether acute inhibition of PI3K

Table 2 Echocardiographic and catheterisation analyses of heart size and function

Variable	Ntg		dnPI3K		caPI3K	
	Non-diabetic	Diabetic	Non-diabetic	Diabetic	Non-diabetic	Diabetic
M-mode echocardiography, *n*	11	11	6	7	6	8
LVPW (mm)	0.88±0.02	0.80±0.03	0.74±0.03*	0.75±0.04*	1.07±0.04*	0.97±0.02*†‡§
LVDD (mm)	3.79±0.07	3.83±0.07	3.74±0.11	3.69±0.19	3.68±0.07	3.75±0.10
LVSD (mm)	2.35±0.05	2.36±0.07	2.47±0.12	2.36±0.21	2.21±0.11	2.07±0.12
Fractional shortening (%)	38±1	38±2	34±2	37±3	40±2	45±2*‡§
Heart rate (bpm)	426±13	450±13	410±20	373±9*‡	426±26	436±10§
Catheterisation, *n*	8	11	5	6	6	7
Heart rate (bpm)	327±7	344±5	309±10	334±20	323±21	368±14
Aortic SBP (mmHg)	98±3	84±3†	101±8	77±2*†	94±4	87±2*
LVSP (mmHg)	99±3	85±2†	95±6	78±2*†	96±3	92±2§
dP/dt_{max} (mmHg/s)	6,610±249	7,266±200	6,784±762	6,432±618	7,401±503	7,906±297
dP/dt_{min} (mmHg/s)	5,330±163	4,686±185†	5,196±434	4,315±270*†	5,335±323	5,222±227§

*$p<0.05$ vs Ntg non-diabetic mice; †$p<0.05$ vs non-diabetic mice of the same genotype; ‡$p<0.05$ vs Ntg diabetic mice; §$p<0.05$ vs dnPI3K diabetic mice

dP/dt_{max}, maximum rate of left ventricular pressure change; LVDD, left ventricular diastolic dimension; LVPW, left ventricular posterior wall; LVSD, left ventricular systolic dimension; LVSP, left ventricular systolic pressure; SBP, systolic blood pressure

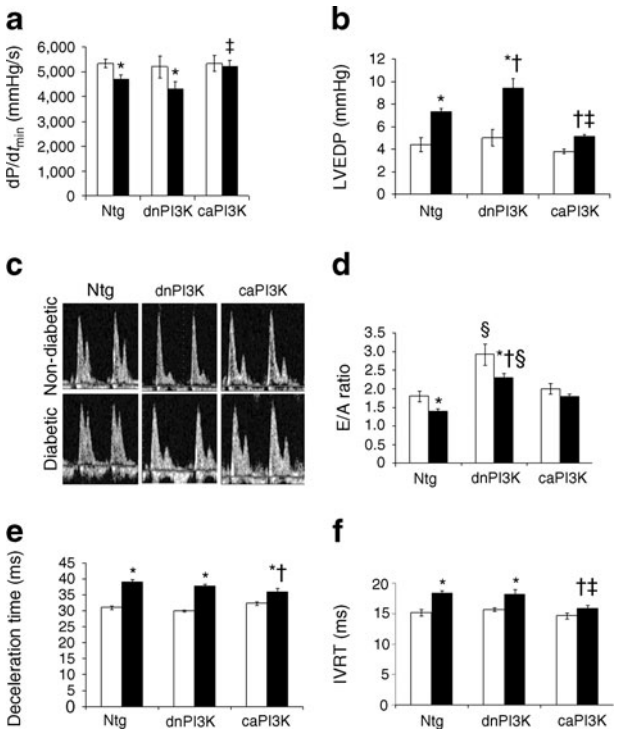

Fig. 3 PI3K(p110α) provides protection against diastolic dysfunction. (**a**) dP/dt_{min} and (**b**) LVEDP assessed by catheterisation; n=5–11 per group. (**c**) Representative mitral flow patterns from pulsed-wave Doppler echocardiography. (**d**) E/A wave ratio, (**e**) deceleration time and (**f**) IVRT. (**c**–**f**) n=4–10 per group. White bars, non-diabetic; black bars, diabetic. *$p\leq0.05$ vs non-diabetic mice of the same genotype; †$p<0.05$ vs diabetic Ntg mice; ‡$p<0.05$ vs diabetic dnPI3K mice; §$p<0.05$ vs non-diabetic and diabetic Ntg mice

(p110α) with a specific inhibitor (A66) would increase superoxide (as occurred in the dnPI3K heart). In NRVM, HG induced an increase in superoxide compared with LG, which was blunted with IGF1 (Fig. 4e), whereas A66 in a setting of HG increased superoxide, which was prevented with tempol (a superoxide dismutase mimetic; Fig. 4f). The more robust H9c2 cell line was studied under HG conditions with and without H_2O_2. The addition of H_2O_2 was designed to mimic the chronic impact of HG causing mitochondrial dysfunction and the subsequent release of mitochondrial ROS (e.g. H_2O_2). Under HG conditions, H_2O_2 and A66 (alone or in combination) all increased superoxide generation and this was blunted by tempol (Fig. 4g). Furthermore, IGF1 treatment suppressed superoxide generation induced by HG with H_2O_2 (Fig. 4h).

Differential NADPH-driven superoxide generation in PI3K-Tg (Fig. 4a) indicates that PI3K regulates extra-mitochondrial ROS. To assess whether PI3K has the potential to regulate mitochondrial function and mitochondrial ROS production, we examined expression of *Tfam* (essential for mitochondrial transcription and replication) and *Ucp3*/UCP3 (a mitochondrial anion carrier protein that can limit mitochondrial ROS production [30]). *Tfam* gene expression was lower in hearts of non-diabetic dnPI3K compared with non-diabetic Ntg mice and there was no change with diabetes (Fig. 5a). By contrast, *Tfam* expression was higher in caPI3K than dnPI3K mice in non-diabetic and diabetic conditions (Fig. 5a). *Ucp3* gene expression and UCP3 protein production tended to increase in a setting of diabetes in each of the genotypes, but were only significantly

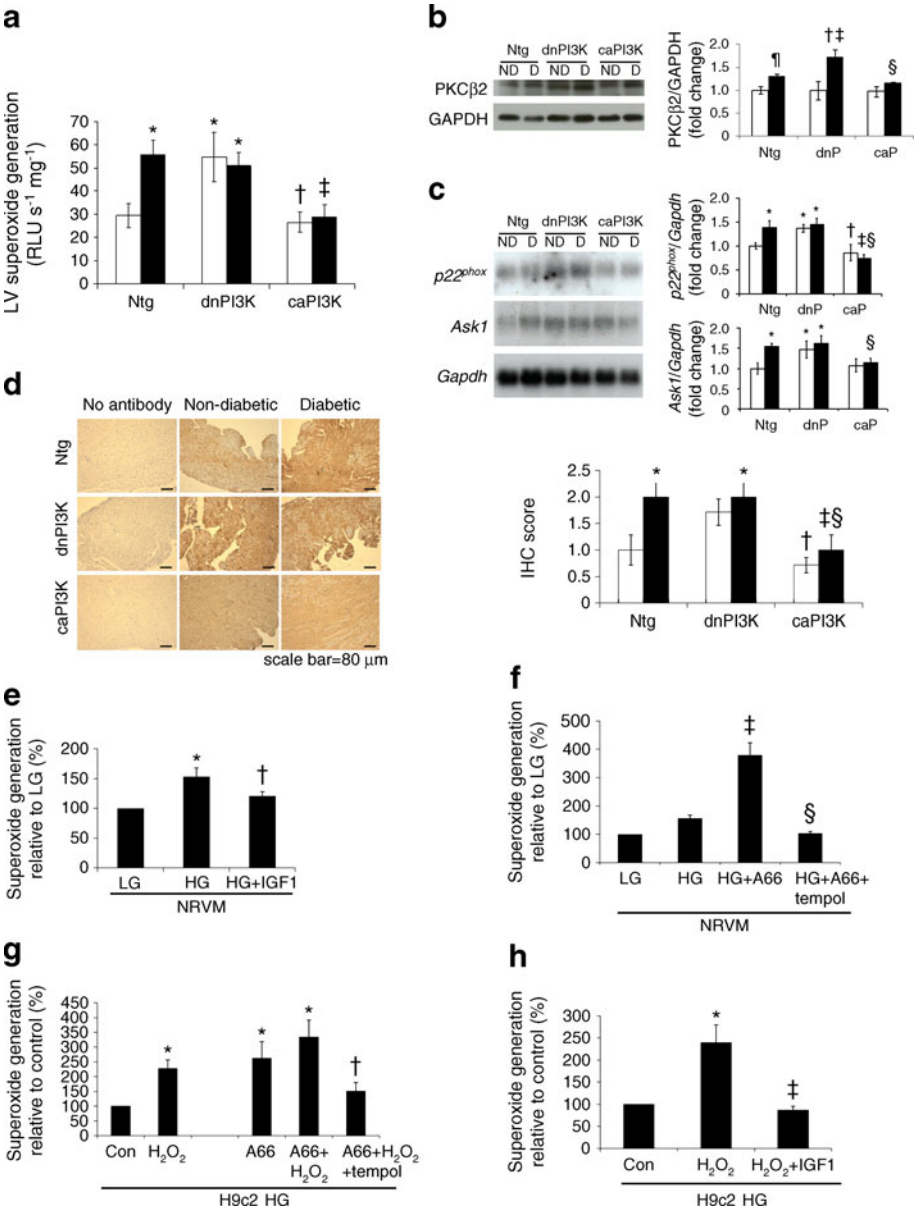

Fig. 4 PI3K(p110α) protects against diabetes-induced superoxide generation. (**a**) LV superoxide generation assessed by lucigenin-enhanced chemiluminescence expressed as relative light units per second per mg (RLU $s^{-1}mg^{-1}$). (**b**) Western blot showing PKCβ2 and GAPDH in hearts of non-diabetic (ND) and diabetic (D) mice, and quantitative analysis of PKCβ2 normalised to GAPDH (n=4–5 per group). (**c**) Representative northern blot showing gene expression of *p22*^{phox} (n=4–6 per group) and *Ask1* (n=5–6 per group) from Ntg, dnPI3K (dnP) and caPI3K (caP) mice. *Gapdh* was used to normalise for RNA loading. Quantitative analyses. Mean values for non-diabetic Ntg mice were normalised to 1. (**d**) Immunohistochemical (IHC) examination of p22^{phox} in LV sections. Representative staining (p22^{phox} stains brown; magnification ×100; scale bars, 80 μm) and semi-quantitative analysis (IHC score; n=3 per group). (**a**–**d**) White bars, non-diabetic; black bars, diabetic. *p<0.05 vs non-diabetic Ntg mice; $^{¶}p$<0.05 vs non-diabetic Ntg mice (unpaired t test); $^{†}p$<0.05 vs non-diabetic dnPI3K mice; $^{‡}p$<0.05 vs diabetic Ntg mice; $^{§}p$<0.05 vs diabetic dnPI3K mice. Superoxide generation in NRVM under LG and HG conditions treated with IGF1 (**e**), A66 (PI3K [p110α] inhibitor) and tempol (superoxide dismutase mimetic) (**f**), n=4–5 per group. *p< 0.05 vs LG; $^{†}p$<0.05 vs HG; $^{‡}p$<0.05 vs LG and HG; $^{§}p$<0.05 vs HG +A66. Superoxide generation in H9c2 cells under HG conditions treated with H_2O_2, A66, tempol (**g**) and IGF1 (**h**) (n=5–7 per group). *p<0.05 vs control; $^{†}p$<0.05 vs A66+H_2O_2; $^{‡}p$<0.05 vs H_2O_2. (**e**–**h**) Statistics performed using one-way repeated measures ANOVA followed by pairwise multiple comparison (Student–Newman–Keuls). Values relative to LG or control (100%) as shown

higher in caPI3K diabetic mice (Fig. 5b, c). To more directly examine whether activation of PI3K can affect mitochondrial function, we measured the respiratory profile of IGF1-treated H9c2 cells under HG conditions with or without the specific PI3K(p110α) inhibitor, A66. IGF1 treatment was associated with increased basal respiration, uncoupled respiration, ATP

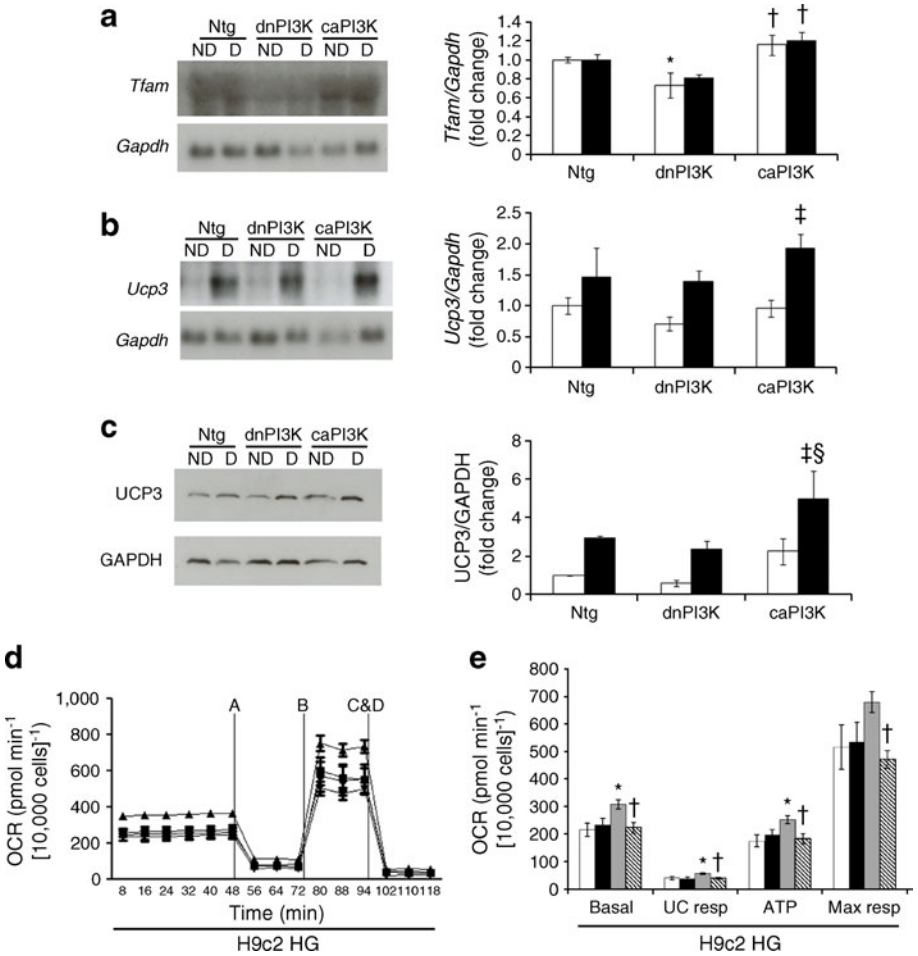

Fig. 5 Enhanced PI3K(p110α) activity increases *Tfam* and *Ucp3*/UCP3 expression and improves mitochondrial function. (**a**, **b**) Representative northern blots showing gene expression of *Tfam* and *Ucp3* in hearts of non-diabetic (ND) and diabetic (D) mice. *Gapdh* was used to normalise for RNA loading. Quantitative analyses (n=3–4 per group). (**c**) Representative western blot showing UCP3 and GAPDH, and quantitative analysis (right panel; n=3 per group). (**a**–**c**) White bars, non-diabetic; black bars, diabetic. Mean values for non-diabetic Ntg mice were normalised to 1. *p<0.05 vs non-diabetic Ntg mice; $^{\dagger}p$<0.05 vs non-diabetic and diabetic dnPI3K mice; $^{\ddagger}p$<0.05 vs non-diabetic mice of the same genotype; $^{\S}p$<0.05 vs diabetic dnPI3K mice. (**d**) Trace of mean data showing oxygen consumption rate (OCR) throughout a mitochondrial function test (A, oligomycin; B, FCCP; C&D, antimycin A and rotenone) in H9c2 cells in HG conditions. Circles (difficult to identify because of overlap), control (HG alone); squares, A66-treated; upward triangles, IGF1-treated; downward triangles, IGF1- and A66-treated. (**e**) Quantitation. ATP, ATP turnover; Max resp, maximal respiration; UC resp, uncoupled respiration. White bars, control (HG alone); black bars, A66; grey bars, IGF1; hatched bars, IGF1 and A66. *p<0.05 vs control; $^{\dagger}p$<0.05 vs IGF1

turnover and a trend towards increased maximal respiration (p<0.06); these changes were all prevented by the PI3K (p110α) inhibitor (Fig. 5d, e).

Discussion

The development of improved therapeutics for patients with diabetic cardiomyopathy will require a comprehensive understanding of the critical mechanisms responsible for the induction and transition to cardiomyopathy in a setting of hyperglycaemia. To our knowledge, this is the first study to show a direct causal role of decreased PI3K activity in exacerbating diabetic cardiomyopathy and increased PI3K activity in preventing diabetic cardiomyopathy. Another key finding from this study is in vivo evidence that PI3K (p110α) regulates superoxide generation in the mouse heart under basal and diabetic settings. The cardiac protection observed in a setting of enhanced PI3K(p110α) activation was associated with increased AKT phosphorylation, *Tfam* and *Ucp3*/UCP3 expression, and suppression of LV superoxide generation, PKCβ2 production, $p22^{phox}$ and *Ask1* expression.

Utilising dnPI3K-Tg mice with depressed PI3K(p110α) activity, we have demonstrated that PI3K(p110α) is critical for protecting the heart against dysfunction and remodelling in a setting of type 1 diabetes. In contrast, increasing PI3K (p110α) activity utilising caPI3K-Tg mice provided protection

against diastolic dysfunction and myocardial remodelling in a diabetes model. LV diastolic dysfunction is one of the earliest manifestations of diabetic cardiomyopathy, presenting prior to the onset of systolic dysfunction [26, 31, 32]. Diastolic dysfunction is characterised by abnormal LV relaxation and filling, associated with elevated LVEDP, a depressed E/A ratio and increased deceleration time [25]. Contributing factors include pathological cardiomyocyte hypertrophy, increased cell death and fibrosis. Previous studies have reported each of these features in the STZ-induced type 1 diabetes mouse model [21, 26, 33]. In the current study, diabetes in Ntg and dnPI3K-Tg mice was associated with a depressed E/A ratio and increased LVEDP, deceleration time, IVRT, myocyte size, apoptosis and fibrosis compared with non-diabetic mice. LVEDP, fibrosis and apoptosis were further elevated in diabetic dnPI3K-Tg compared with diabetic Ntg mice. By contrast, diabetes was not associated with changes in LVEDP, E/A ratio, IVRT, myocyte size, fibrosis or apoptosis in caPI3K-Tg mice.

Oxidative stress contributes to the cardiovascular complications associated with diabetes [34]. NADPH oxidase generates superoxide and is considered a major source of ROS in the heart [9, 35]. In the current study, NADPH-driven superoxide generation was increased in diabetic Ntg hearts compared with non-diabetic Ntg hearts, and this was accompanied by increased production of a membrane-associated subunit of NADPH oxidase ($p22^{phox}$). The $p22^{phox}$ NADPH subunit was the focus of this study because it was the only subunit that was differentially regulated in the hearts of PI3K-Tg mice under control or sham conditions based on previous microarray data [12]. Interestingly, superoxide generation and *p22*^{phox} in the current study were higher in hearts from non-diabetic dnPI3K compared with non-diabetic Ntg mice, and remained elevated in a setting of diabetes. By contrast, there was no increase in superoxide production or *p22*^{phox} expression in hearts of non-diabetic and diabetic caPI3K-Tg mice. Findings in the diabetic setting were consistent with those obtained in NRVM and H9c2 cells under HG conditions. In a setting of HG, superoxide generation was enhanced in cells when PI3K(p110α) was inhibited with A66, and blunted when PI3K(p110α) was activated with IGF1. Tempol, a superoxide dismutase mimetic, attenuated A66-induced superoxide generation. Collectively, these data suggest that increased PI3K(p110α) activity mediates protection, at least in part, via attenuation or prevention of superoxide generation.

Our assessment of NADPH-driven superoxide generation indicates that PI3K regulates extra-mitochondrial ROS. Tissue availability constraints precluded direct measurements of mitochondrial ROS. However, to assess the potential contribution of mitochondria, we examined cardiac *Tfam* and *Ucp3* expression/UCP3 production, and performed a mitochondrial function test in H9c2 cells in HG conditions. *Tfam* and *Ucp3* expression/UCP3 production were elevated in hearts of diabetic caPI3K mice, and acute activation of the IGF1–PI3K(p110α) pathway in H9c2 cells enhanced mitochondrial function in a setting of HG. Collectively, this could contribute to the protection observed in diabetic caPI3K mice. UCP3 can protect muscle cells against mitochondrial ROS and oxidative damage [30], and overexpression of *Tfam* protected the heart against mitochondrial respiratory defects and cardiac dysfunction in a setting of myocardial infarction [36]. In addition, it was previously shown that isolated mitochondria from caPI3K mice (basal conditions) had increased mitochondrial enzymatic activity, associated with increased fatty acid oxidative capacity [37].

Under basal/non-diabetic conditions, dnPI3K-Tg mice have normal cardiac function despite increased cardiac expression of *p22*^{phox} and *Ask1*, decreased *Tfam* and increased LV superoxide generation. We recently reported that genes encoding key components of the Z-disc are also depressed in hearts of dnPI3K mice [38]. This suggests that the dnPI3K heart can compensate for these abnormalities under normal conditions but not under conditions of stress such as diabetes, resulting in accelerated cardiomyopathy. Consistent with this hypothesis, cardiac-specific *Ask1*-Tg mice show no evidence of pathology under basal conditions, but display a more severe pathological phenotype (cardiac dysfunction, increased fibrosis and apoptosis) in response to pressure overload or ischaemia–reperfusion injury [39]. Furthermore, basal blood pressure was normal in *Nox2*-Tg mice despite increased vascular ROS production and increased $p22^{phox}$ protein. Differences in blood pressure compared with wild-type mice were only apparent in response to an insult (angiotensin II infusion) [40].

Based on data presented in the current study, together with previous reports in the literature, we have assembled a schematic highlighting mechanisms via which increased PI3K(p110α) could mediate protection in a setting of diabetes (Fig. 6). It is well recognised that hyperglycaemia causes activation of PKCβ2 in the heart and subsequent activation of NADPH oxidase [29]. In the current study, PKCβ2 production and *p22*^{phox} expression were increased in diabetic Ntg hearts but not diabetic caPI3K hearts. PKCβ2 can phosphorylate $p22^{phox}$ [41], and we previously demonstrated that the ca*PI3K* transgene can blunt cardiac pathology and PKCβ2 protein production in PKCβ2-Tg mice [42]. Superoxide generation, *Ask1* expression and apoptosis were elevated in hearts of diabetic Ntg and dnPI3K-Tg mice, but not in diabetic caPI3K-Tg mice. Increased pAKT was maintained in hearts of diabetic caPI3K-Tg mice, and AKT was previously shown to directly inhibit apoptosis

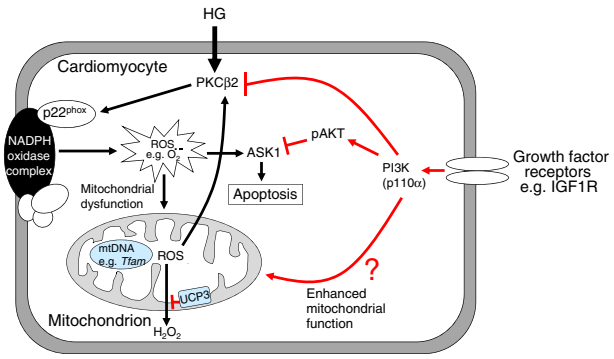

Fig. 6 Proposed mechanisms via which PI3K(p110α) could mediate protection in a setting of HG. HG activates PKCβ2 in the heart, leading to activation of NADPH oxidase. ROS (e.g. superoxide, $O_2^{\bullet-}$) produced by NADPH oxidase causes mitochondrial dysfunction and increased mitochondrial ROS, which can cause further activation of PKCβ2. ROS activates ASK1 leading to apoptosis. Protective properties of PI3K(p110α) are highlighted in red. Further studies will be required to assess whether PI3K(p110α) can enhance mitochondrial function in a setting of diabetes in vivo

signal-regulating kinase 1 (ASK1) in response to oxidative stress [43]. Further, AKT1 or deficiency of ASK1 protects the heart against cardiac pathology [44–46]. Thus, PI3K (p110α) is likely to mediate protection, in part, by activation of AKT. NADPH oxidase-induced ROS production can lead to mitochondrial dysfunction and increased mitochondrial ROS. Increased expression/production of *Ucp3*/UCP3 and *Tfam* in diabetic caPI3K hearts, together with enhanced mitochondrial function in IGF1-treated H9c2 cells in HG conditions, may suggest that PI3K(p110α) is able to enhance mitochondrial function in a setting of diabetes. However, this will require further investigation.

Limitations and future research Limited tissue availability precluded a thorough assessment of apoptosis mechanisms (mitochondrial vs extra-mitochondrial), other NADPH oxidase subunits (activation and translocation, e.g. *Nox2* has previously been implicated in a setting of hyperglycaemia [47]) and activity of PKCβ2, PIM1 and ASK1. Such assessment will be important to more comprehensively understand why the dnPI3K heart progresses to cardiomyopathy in a setting of diabetes but not under basal conditions, despite elevated expression of some ROS-related genes and superoxide in both settings. While results obtained from NRVM with or without the PI3K(p110α) inhibitor were similar to those obtained in hearts from diabetic dnPI3K-Tg mice, it is acknowledged that pharmacological inhibitors are generally less specific than genetic tools, and the metabolism of NRVM is different from adult cells. Caution should also be taken when comparing results from in vitro, ex vivo and in vivo studies, as mechanisms may differ. The isolation of mitochondria from PI3K-Tg mice under diabetic conditions will be important to comprehensively examine the role of PI3K(p110α) in regulating mitochondrial function and mitochondrial ROS.

The current study suggests that increasing PI3K(p110α) activity in the heart could prevent LV superoxide generation and diabetic cardiomyopathy. We recently generated a recombinant adeno-associated viral (rAAV) vector containing caPI3K that selectively transduced cardiac muscle, minimising the concern of PI3K's tumorigenic potential in other cell types [48]. rAAV6–caPI3K improved cardiac function in a mouse model of pressure overload and AAV-based therapies have entered clinical trials in heart failure patients [49, 50]. Future studies will be required to assess whether rAAV6–caPI3K can improve function in a setting of diabetic cardiomyopathy.

In summary, we have shown that increasing PI3K (p110α) in the hearts of STZ-induced type 1 diabetic mice provided protection against diastolic dysfunction, cardiomyocyte hypertrophy, cardiac fibrosis and apoptosis. By contrast, decreasing PI3K(p110α) in type 1 diabetic mice was associated with accelerated cardiomyopathy. Enhanced PI3K(p110α) activity prevented a diabetes-induced increase in LV superoxide generation, PKCβ2 production, and *p22^{phox}* and *Ask1* expression. Furthermore, activation of PI3K(p110α) in cardiomyocyte-like cells was able to suppress HG-induced superoxide generation and enhance mitochondrial function. Thus, therapies that target the cardiac PI3K(p110α) pathway may represent a potential strategy for the prevention and treatment of cardiomyopathy in diabetic patients.

Acknowledgements The authors thank T. Julius, N. Jennings, A. Matsumoto, J.W. Tan, P. Chew and L. Lim (all from the Baker IDI Heart and Diabetes Institute) for technical assistance with echocardiography, immunohistochemistry and molecular analyses.

Funding This work was supported by a National Health and Medical Research Council (NHMRC) of Australia project grant (ID526638 to RHR, JRM and KJD), and supported in part by the Victoria Government's Operational Infrastructure Support Program. KH is supported by an Australian Postgraduate Award. DCH is supported by a National Heart Foundation Fellowship (PF 10M 5347). RHR, KJD, XJD and JRM are NHMRC Senior Research Fellows (IDs 472673, 526605, 317808 and 586604). JRM is supported by an Australia Research Council Future Fellowship (FT0001657).

Duality of interest The authors declare that there is no duality of interest associated with this manuscript.

Contribution statement RHR contributed to the design of the study, data acquisition, analysis and interpretation of data, and revising it critically for important intellectual content. JEL, KH, BCB and DCH contributed to the design of some experiments, data acquisition and interpretation, and manuscript revision. HK, YKT, GS, NC, CQ and EJHB contributed to data acquisition and interpretation, and manuscript revision. KJD and XJD contributed to design of the study, data interpretation and revising it critically for important intellectual content. JRM contributed to the design of the study, data acquisition, analysis and interpretation of data, and drafting the article. All authors approved the final version of the manuscript.

References

1. Shaw JE, Sicree RA, Zimmet PZ (2009) Global estimates of the prevalence of diabetes for 2010 and 2030. Diabetes Res Clin Pract 87:4–14
2. Lancet (2011) The diabetes pandemic. Lancet 378:99
3. Devereux RB, Roman MJ, Paranicas M et al (2000) Impact of diabetes on cardiac structure and function: the strong heart study. Circulation 101:2271–2276
4. Boudina S, Abel ED (2007) Diabetic cardiomyopathy revisited. Circulation 115:3213–3223
5. He X, Kan H, Cai L, Ma Q (2009) Nrf2 is critical in defense against high glucose-induced oxidative damage in cardiomyocytes. J Mol Cell Cardiol 46:47–58
6. Giugliano D, Ceriello A, Paolisso G (1995) Diabetes mellitus, hypertension, and cardiovascular disease: which role for oxidative stress? Metabolism 44:363–368
7. Meigs JB, Larson MG, Fox CS, Keaney JF Jr, Vasan RS, Benjamin EJ (2007) Association of oxidative stress, insulin resistance, and diabetes risk phenotypes: the Framingham Offspring Study. Diabetes Care 30:2529–2535
8. Cai L, Kang YJ (2001) Oxidative stress and diabetic cardiomyopathy: a brief review. Cardiovasc Toxicol 1:181–193
9. Li JM, Gall NP, Grieve DJ, Chen M, Shah AM (2002) Activation of NADPH oxidase during progression of cardiac hypertrophy to failure. Hypertension 40:477–484
10. Schramm TK, Gislason GH, Vaag A et al (2011) Mortality and cardiovascular risk associated with different insulin secretagogues compared with metformin in type 2 diabetes, with or without a previous myocardial infarction: a nationwide study. Eur Heart J 32:1900–1908
11. Discov NRD (2009) Regulatory watch: FDA issues guidance for cardiovascular risk assessment of novel antidiabetic agents. Nat Rev Drug Discov 8:99
12. Lin RC, Weeks KL, Gao XM et al (2010) PI3K (p110 alpha) protects against myocardial infarction-induced heart failure: identification of PI3K-regulated miRNA and mRNA. Arterioscler Thromb Vasc Biol 30:724–732
13. McMullen JR, Amirahmadi F, Woodcock EA et al (2007) Protective effects of exercise and phosphoinositide 3-kinase (p110alpha) signaling in dilated and hypertrophic cardiomyopathy. Proc Natl Acad Sci USA 104:612–617
14. Pretorius L, Du XJ, Woodcock EA et al (2009) Reduced phosphoinositide 3-kinase (p110alpha) activation increases the susceptibility to atrial fibrillation. Am J Pathol 175:998–1009
15. Lee YJ, Lee JH, Han HJ (2006) Extracellular adenosine triphosphate protects oxidative stress-induced increase of p21 (WAF1/Cip1) and p27 (Kip1) expression in primary cultured renal proximal tubule cells: role of PI3K and Akt signaling. J Cell Physiol 209:802–810
16. Kuo WW, Chung LC, Liu CT et al (2009) Effects of insulin replacement on cardiac apoptotic and survival pathways in streptozotocin-induced diabetic rats. Cell Biochem Funct 27:479–487
17. Gross ER, Hsu AK, Gross GJ (2007) Diabetes abolishes morphine-induced cardioprotection via multiple pathways upstream of glycogen synthase kinase-3beta. Diabetes 56:127–136
18. Miki T, Miura T, Hotta H et al (2009) Endoplasmic reticulum stress in diabetic hearts abolishes erythropoietin-induced myocardial protection by impairment of phospho-glycogen synthase kinase-3beta-mediated suppression of mitochondrial permeability transition. Diabetes 58:2863–2872
19. Tsang A, Hausenloy DJ, Mocanu MM, Carr RD, Yellon DM (2005) Preconditioning the diabetic heart: the importance of Akt phosphorylation. Diabetes 54:2360–2364
20. Shioi T, Kang PM, Douglas PS et al (2000) The conserved phosphoinositide 3-kinase pathway determines heart size in mice. EMBO J 19:2537–2548
21. Huynh K, McMullen JR, Julius TL et al (2010) Cardiac-specific IGF-1 receptor transgenic expression protects against cardiac fibrosis and diastolic dysfunction in a mouse model of diabetic cardiomyopathy. Diabetes 59:1512–1520
22. Laskowski A, Woodman OL, Cao AH et al (2006) Antioxidant actions contribute to the antihypertrophic effects of atrial natriuretic peptide in neonatal rat cardiomyocytes. Cardiovasc Res 72:112–123
23. Jamieson S, Flanagan JU, Kolekar S et al (2011) A drug targeting only p110alpha can block phosphoinositide 3-kinase signalling and tumour growth in certain cell types. Biochem J 438:53–62
24. Asbun J, Villarreal FJ (2006) The pathogenesis of myocardial fibrosis in the setting of diabetic cardiomyopathy. J Am Coll Cardiol 47:693–700
25. Asghar O, Al-Sunni A, Khavandi K et al (2009) Diabetic cardiomyopathy. Clin Sci (Lond) 116:741–760
26. Kajstura J, Fiordaliso F, Andreoli AM et al (2001) IGF-1 overexpression inhibits the development of diabetic cardiomyopathy and angiotensin II-mediated oxidative stress. Diabetes 50:1414–1424
27. Anilkumar N, Sirker A, Shah AM (2009) Redox sensitive signaling pathways in cardiac remodeling, hypertrophy and failure. Front Biosci 14:3168–3187
28. Ritchie RH, Irvine JC, Rosenkranz AC et al (2009) Exploiting cGMP-based therapies for the prevention of left ventricular hypertrophy: NO* and beyond. Pharmacol Ther 124:279–300
29. Geraldes P, King GL (2010) Activation of protein kinase C isoforms and its impact on diabetic complications. Circ Res 106:1319–1331
30. Costford SR, Seifert EL, Bezaire V et al (2007) The energetic implications of uncoupling protein-3 in skeletal muscle. Appl Physiol Nutr Metab 32:884–894
31. Schannwell CM, Schneppenheim M, Perings S, Plehn G, Strauer BE (2002) Left ventricular diastolic dysfunction as an early manifestation of diabetic cardiomyopathy. Cardiology 98:33–39
32. Karamitsos TD, Karvounis HI, Dalamanga EG et al (2007) Early diastolic impairment of diabetic heart: the significance of right ventricle. Int J Cardiol 114:218–223
33. Wold LE, Ceylan-Isik AF, Fang CX et al (2006) Metallothionein alleviates cardiac dysfunction in streptozotocin-induced diabetes: role of Ca^{2+} cycling proteins, NADPH oxidase, poly (ADP-Ribose) polymerase and myosin heavy chain isozyme. Free Radic Biol Med 40:1419–1429
34. Haidara MA, Yassin HZ, Rateb M, Ammar H, Zorkani MA (2006) Role of oxidative stress in development of cardiovascular complications in diabetes mellitus. Curr Vasc Pharmacol 4:215–227
35. MacCarthy PA, Grieve DJ, Li JM, Dunster C, Kelly FJ, Shah AM (2001) Impaired endothelial regulation of ventricular relaxation in cardiac hypertrophy: role of reactive oxygen species and NADPH oxidase. Circulation 104:2967–2974
36. Ikeuchi M, Matsusaka H, Kang D et al (2005) Overexpression of mitochondrial transcription factor a ameliorates mitochondrial deficiencies and cardiac failure after myocardial infarction. Circulation 112:683–690
37. O'Neill BT, Kim J, Wende AR et al (2007) A conserved role for phosphatidylinositol 3-kinase but not Akt signaling in mitochondrial adaptations that accompany physiological cardiac hypertrophy. Cell Metab 6:294–306
38. Waardenberg AJ, Bernardo BC, Ng DC et al (2011) Phosphoinositide 3-kinase (PI3K (p110alpha)) directly regulates key components of the Z-disc and cardiac structure. J Biol Chem 286:30837–30846

39. Liu Q, Sargent MA, York AJ, Molkentin JD (2009) ASK1 regulates cardiomyocyte death but not hypertrophy in transgenic mice. Circ Res 105:1110–1117
40. Bendall JK, Rinze R, Adlam D et al (2007) Endothelial Nox2 overexpression potentiates vascular oxidative stress and hemodynamic response to angiotensin II: studies in endothelial-targeted Nox2 transgenic mice. Circ Res 100:1016–1025
41. Regier DS, Waite KA, Wallin R, McPhail LC (1999) A phosphatidic acid-activated protein kinase and conventional protein kinase C isoforms phosphorylate p22 (phox), an NADPH oxidase component. J Biol Chem 274:36601–36608
42. Rigor DL, Bodyak N, Bae S et al (2009) Phosphoinositide 3-kinase Akt signaling pathway interacts with protein kinase C{beta}2 in the regulation of physiologic developmental hypertrophy and heart function. Am J Physiol Heart Circ Physiol 296: H566–H572
43. Kim AH, Khursigara G, Sun X, Franke TF, Chao MV (2001) Akt phosphorylates and negatively regulates apoptosis signal-regulating kinase 1. Mol Cell Biol 21:893–901
44. DeBosch B, Treskov I, Lupu TS et al (2006) Akt1 is required for physiological cardiac growth. Circulation 113:2097–2104
45. Yamaguchi O, Higuchi Y, Hirotani S et al (2003) Targeted deletion of apoptosis signal-regulating kinase 1 attenuates left ventricular remodeling. Proc Natl Acad Sci USA 100:15883–15888
46. Izumiya Y, Kim S, Izumi Y et al (2003) Apoptosis signal-regulating kinase 1 plays a pivotal role in angiotensin II-induced cardiac hypertrophy and remodeling. Circ Res 93:874–883
47. Balteau M, Tajeddine N, de Meester C et al (2011) NADPH oxidase activation by hyperglycaemia in cardiomyocytes is independent of glucose metabolism but requires SGLT1. Cardiovasc Res 92:237–246
48. McMullen JR, Jay PY (2007) PI3K (p110alpha) inhibitors as anticancer agents: minding the heart. Cell Cycle 6:910–913
49. Jessup M, Greenberg B, Mancini D et al (2011) Calcium Upregulation by Percutaneous Administration of Gene Therapy in Cardiac Disease (CUPID): a phase 2 trial of intracoronary gene therapy of sarcoplasmic reticulum Ca2 + −ATPase in patients with advanced heart failure. Circulation 124:304–313
50. Weeks KL, Gao X, Du XJ et al (2012) Phosphoinositide 3-kinase p110alpha is a master regulator of exercise-induced cardioprotection and PI3K gene therapy rescues cardiac dysfunction. Circ Heart Fail 5:523–534